

Supporting Information

An easily available lysosomal-targeted ratiometric fluorescent probe with aggregation induced emission characteristics for hydrogen polysulfides visualization in acute ulcerative colitis

Chunbai Xiang†, ^{a, b} Chunbin Li†, ^c Jingjing Xiang†, ^{a, b} Yuan Luo, ^a Jiaofeng Peng, ^d Guanjun Deng, ^a Jianguo Wang, ^c Safacan Kolemen, ^e Hongchun Li, ^f Pengfei Zhang*, ^a Ping Gong*, ^a and Lintao Cai* ^a

a. Guangdong Key Laboratory of Nanomedicine, CAS Key Laboratory of Health Informatics, Shenzhen Bioactive Materials Engineering Lab for Medicine, Institute of Biomedicine and Biotechnology, Shenzhen Institute of Advanced Technology, Chinese Academy of Sciences, Shenzhen 518055, China. *E-mail: pf.zhang@siat.ac.cn, ping.gong@siat.ac.cn and lt.cai@siat.ac.cn

b. University of Chinese Academy of Sciences, Beijing 100049, China.

c. College of Chemistry and Chemical Engineering, Inner Mongolia University, Hohhot 010021, P. R. China.

d. Instrumental Analysis Center of Shenzhen University, Shenzhen University, Shenzhen, 518055, P. R. China.

e. Koc University, Department of Chemistry, Rumelifeneri Yolu, Sariyer, Istanbul, 34450, Turkey.

f. Research Center for Computer-Aided Drug Discovery, Shenzhen Institute of Advanced Technology, Chinese Academy of Sciences, Shenzhen 518055, China.

† These authors contributed equally to this work.

*Corresponding authors:

Prof. Lintao Cai (lt.cai@siat.ac.cn);

Prof. Ping Gong (ping.gong@siat.ac.cn);

Dr. Pengfei Zhang (pf.zhang@siat.ac.cn).

Experiment section

Chemicals and Materials

All reagents and chemicals were purchased from commercial source and used without further purification, GSSH was bought from Wuhan Biocar biomedical Co., Ltd. Solvents and other common reagents were obtained from Energy Chemical. Phosphate buffer saline (pH=7.4) was used to prepare all aqueous solutions. Solution of $S_2O_5^{2-}$, ClO^- , H_2O_2 , MnO_4^- , Mg^{2+} , K^+ , Fe^{3+} , S^{2-} , HSO_3^- , SO_4^{2-} , I^- , $S_2O_8^{2-}$, NO_3^- were prepared by dissolving their chlorides salts in HPLC grade DMSO. The stock solutions of various small biological molecules were prepared from analytically pure chemical reagents. Hydroxyl radical ($\bullet OH$) was generated by reaction of $50 \mu M Fe^{2+}$ with $50 \mu M H_2O_2$. Hydrogen peroxide (H_2O_2) and hypochlorite (ClO^-) were delivered from 30% and 5% aqueous solutions. BALB/C (4–6 weeks old and weighted 18–30 g) and C57BL/6J mice (7–8 weeks old and weighted 20–30 g) were purchased from Vital River Laboratory Animal Technology Co. Ltd (Beijing, China) and all animals received care in compliance with the guidelines outlined in the Guide for the Care and Use of Laboratory Animals. The procedures were approved by Shenzhen Institutes of Advanced Technology, Chinese Academy of Sciences Animal Care and Use Committee.

Instruments

1H NMR and ^{13}C NMR spectra were measured on a Bruker ARX 400 MHz spectrometer. High-resolution mass spectra (HRMS) were recorded on a GCT Premier CAB 048 mass spectrometer operating in MALDI-TOF mode. UV-vis absorption spectra were recorded on a Rarian 50 Conc UV-Visible spectrophotometer. Fluorescence emission spectra were recorded on Edinburgh FS5 fluorescence spectrophotometer. Cellular imaging experiments were performed with confocal laser scanning microscope (LSM 900 with Airyscan2, Zeiss, Germany). In vivo imaging of H_2S_n in live mice was performed on VISQUE® In Vivo Smart-LF imaging system. The quantum yield of TCFPB- H_2S_n and TCFIS was evaluated with absolute PL Quantam Yielded Spectrometer C11347 (HAMAMATSU, Japan).

The Synthesis of TCFIS

99.5mg of 2-(3-cyano-4,5,5-trimethyl-5H-furan-2-ylidene) malononitrile (compound 1, 0.5 mmol), 4-(diethylamino) salicylaldehyde (compound 2, 115.5 mg, 0.6 mmol) and piperidine (14 μ L, 0.3 mmol) was mixed in 10 mL ethanol, The reaction was refluxed overnight, cooled to room temperature, and purified by silica gel chromatography with the mixed solvent of PE/EA (5:1~1:1, v/v) to give TCFIS as a purple solid (159 mg, 85%). 1H NMR (400 MHz, DMSO- d_6) δ 10.87 (s, 1H), 8.24 (s, 1H), 7.70 (d, J = 9.2 Hz, 1H), 6.94 (d, J = 15.2 Hz, 1H), 6.45 (dd, J = 9.3, 2.4 Hz, 1H), 6.15 (d, J = 2.4 Hz, 1H), 3.46 (q, J = 7.1 Hz, 4H), 1.70 (s, 6H), 1.16 (t, J = 7.0 Hz, 6H). ^{13}C NMR (101 MHz, DMSO- d_6) δ 177.97, 175.75, 162.69, 154.55, 114.55, 113.67, 113.30, 112.47, 107.25, 97.67, 96.93, 49.26, 45.04, 26.43, 13.14. HRMS (MALDI-TOF): m/z : $[M+Na]$ calcd for $C_{22}H_{22}N_4O_2Na$: 397.16405; found: 397.16354.

The Synthesis of TCFPB- H_2S_n

TCFIS (100 mg, 0.27 mmol), 2-fluoro-5-nitrobenzoic acid (93mg, 0.5mmol), and 4-dimethylaminopyridine (6 mg, 0.05 mmol) were dispersed in anhydrous CH_2Cl_2 , and then 1-(3-(dimethylamino) propyl) -3- ethylcarbodiimide hydrochloride (67 mg, 0.35 mmol) was added. The reaction was stirred at room temperature for 12 h. The solvent was removed under reduced pressure, and the crude product was purified by with the mixed solvent of PE/EA (6:1~3:1, v/v)

to give TCFPB-H₂S_n as a purple solid (121mg, 83%). ¹H NMR (400 MHz, DMSO-d₆) δ 8.87 (dd, J = 5.9, 2.9 Hz, 1H), 8.65 (dd, J = 8.0, 4.2 Hz, 1H), 8.15 – 8.07 (m, 2H), 7.77 (t, J = 9.5 Hz, 1H), 6.97 – 6.83 (m, 3H), 3.52 (q, J = 7.0 Hz, 4H), 1.67 (s, 6H), 1.17 (t, J = 7.0 Hz, 6H). ¹³C NMR (101 MHz, DMSO-d₆) δ 178.08, 175.71, 166.68, 164.00, 153.26, 153.19, 144.15, 141.90, 131.85, 131.65, 128.56, 119.98, 119.73, 114.21, 113.82, 112.89, 111.35, 109.87, 105.89, 98.86, 91.85, 51.84, 45.00, 25.51, 13.01. HRMS (MALDI-TOF): m/z: [M+Na] calcd for C₂₉H₂₄N₅O₅FNa: 564.16592; found: 564.16553.

Photostability

To investigate the photostability of the probe system, the PL intensities of TCFPB-H₂S_n (*I*_{619 nm}) in PBS solution were monitored by an Edinburgh FS5 fluorescence spectrophotometer, upon continuous irradiation with a 150 W Xe light (575 nm) of the fluorescence spectrophotometer, respectively. The photostability of TCFPB-H₂S_n was demonstrated by plotting *I*/*I*₀ versus the irradiation time, where *I* is the PL intensity of TCFPB-H₂S_n after the irradiation time of *t*, and *I*₀ is the PL intensity of TCFPB-H₂S_n before light irradiation.

General procedures for the detection of H₂S_n

Unless otherwise noted, all the spectral measurements were performed in 5 mM phosphate buffer (pH 7.4, containing 0.5% DMSO) according to the following procedure. H₂S_n was prepared from Na₂S₄ in aqueous solution. The stock solution (1.0 mM) of probe TCFPB-H₂S_n was first prepared in DMSO. 10 μL of TCFPB-H₂S_n stock solution was added to 2 mL PBS followed by addition of different volume of H₂S_n solution. The mixture was incubated at 37°C, and the reaction solution was transferred to a quartz cell with an optical length of 1 cm for measurement.

Determination of the detection limit of TCFPB-H₂S_n toward addition of H₂S_n

Based on the linear fitting in Figure 2C, the detection limit (*C*) is estimated as follows:

$$C = 3\sigma/K$$

Where σ is the standard deviation obtained from three individual fluorescent intensity ratio (*I*_{619nm}/*I*_{751nm}) of TCFPB-H₂S_n (5 μM) without any H₂S_n and *K* is the slope obtained after linear fitting the titration curves in Figure 2C.

Cell Culture

The HeLa cells were cultured in DMEM (containing 10% heat-inactivated FBS, 100 mg·mL⁻¹ penicillin and 100 mg·mL⁻¹ streptomycin) at 37 °C in a humidified incubator with 5% CO₂. Before the experiments, the cells were precultured until confluence was reached.

Fluorescence Imaging in the acute ulcerative colitis Mice

The 8week-old-female C57BL/6J mice were divided into two groups. The first group was a control group that was kept by drinking distilled water. The second group drank 3% DSS for 1 week. All mice were then injected with 100 μL of PBS containing 1 μM TCFPB-H₂S_n, and the images were obtained by a small animal optical in vivo imaging system. Histological analysis was performed on sacrificed mice after the in vivo imaging. The colon was immobilized in a 4% paraformaldehyde solution and embedded in paraffin wax. Colonic tissue was stained with eosin (H&E) and then examined under a light microscope.

Computational Methods Details

We used GaussView 5.0¹ and Gaussian 09² software for structural visualization and simulation respectively. The structure of the compound is optimized to obtain the minimum energy form. The B3LYP function of DFT is implemented in the current research. For orbitals description, Pople basis set' 6-31G(d) is used for carbon, hydrogen, nitrogen, fluorine and oxygen atoms. Generate the highest occupied molecular orbitals (HOMOs) and lowest unoccupied molecular orbitals (LUMOs) to understand the electron density distribution of all compounds.

Figures and tables

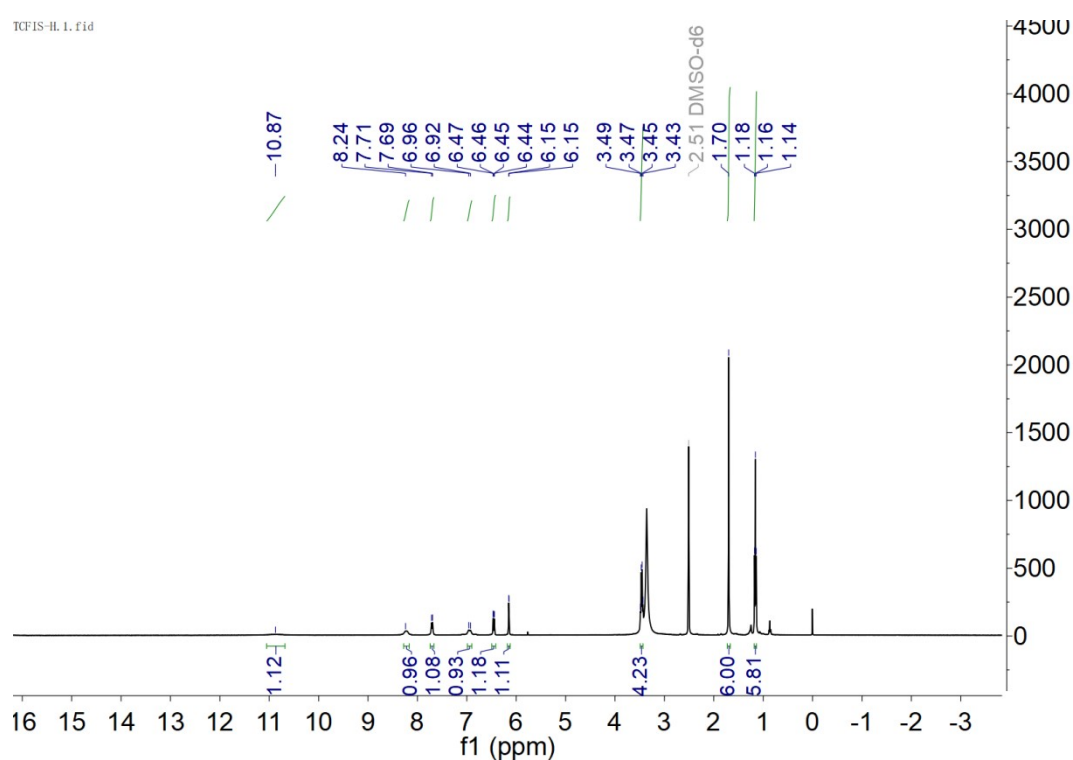


Figure S1. ¹H NMR spectrum of TCFIS in *d*₆-DMSO.

TCFIS-H-C.3.fid

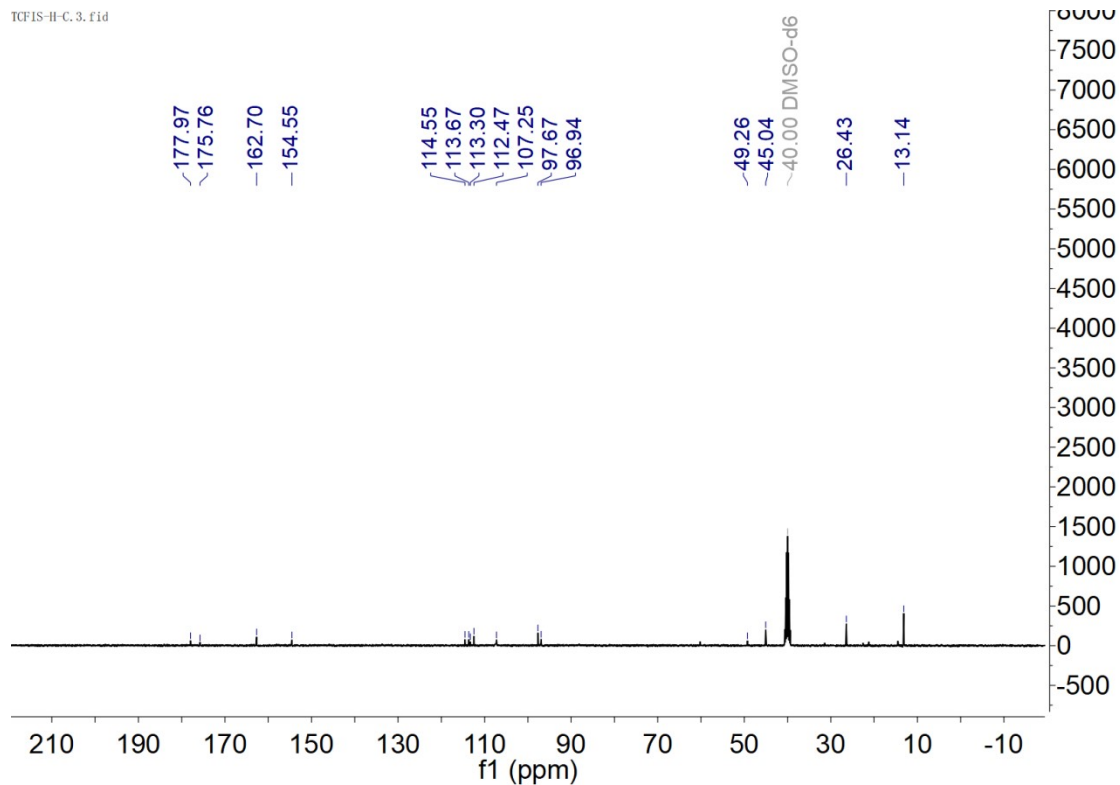


Figure S2. ^{13}C NMR spectrum of TCFIS in d_6 -DMSO.

TCFPB-H.2.fid

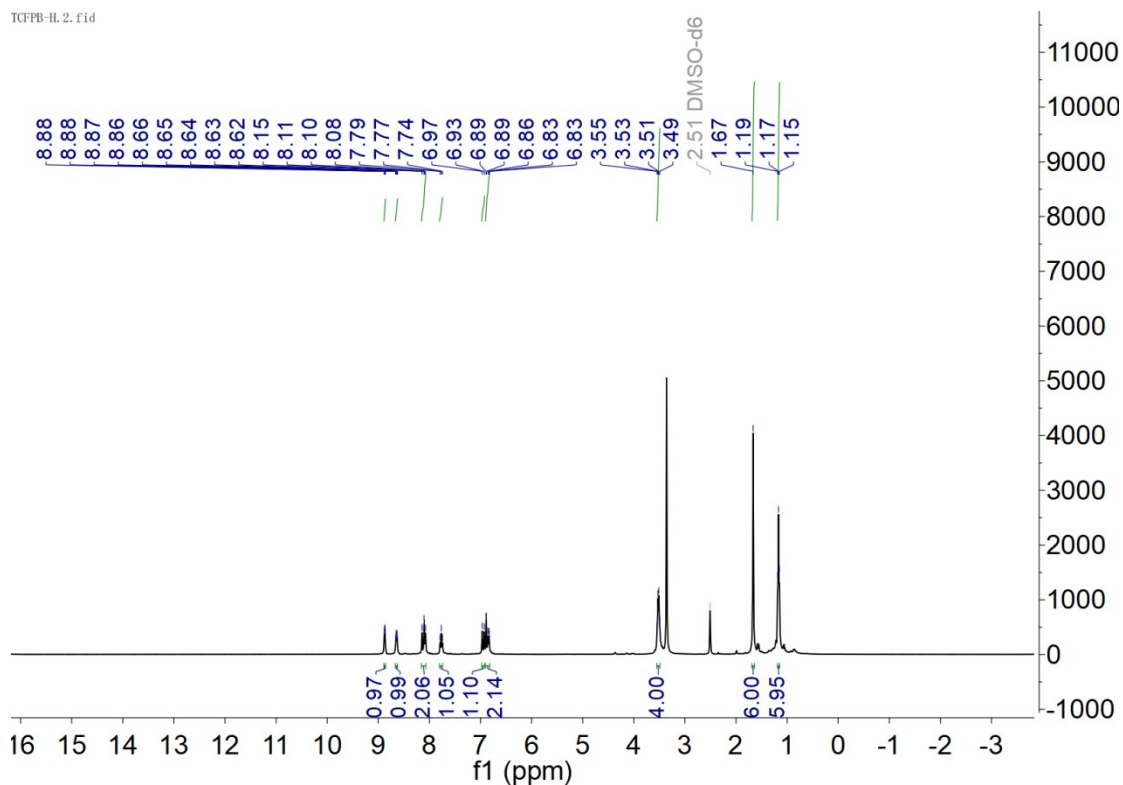


Figure S3. ^1H NMR spectrum of TCFPB- H_2S_n in d_6 -DMSO.

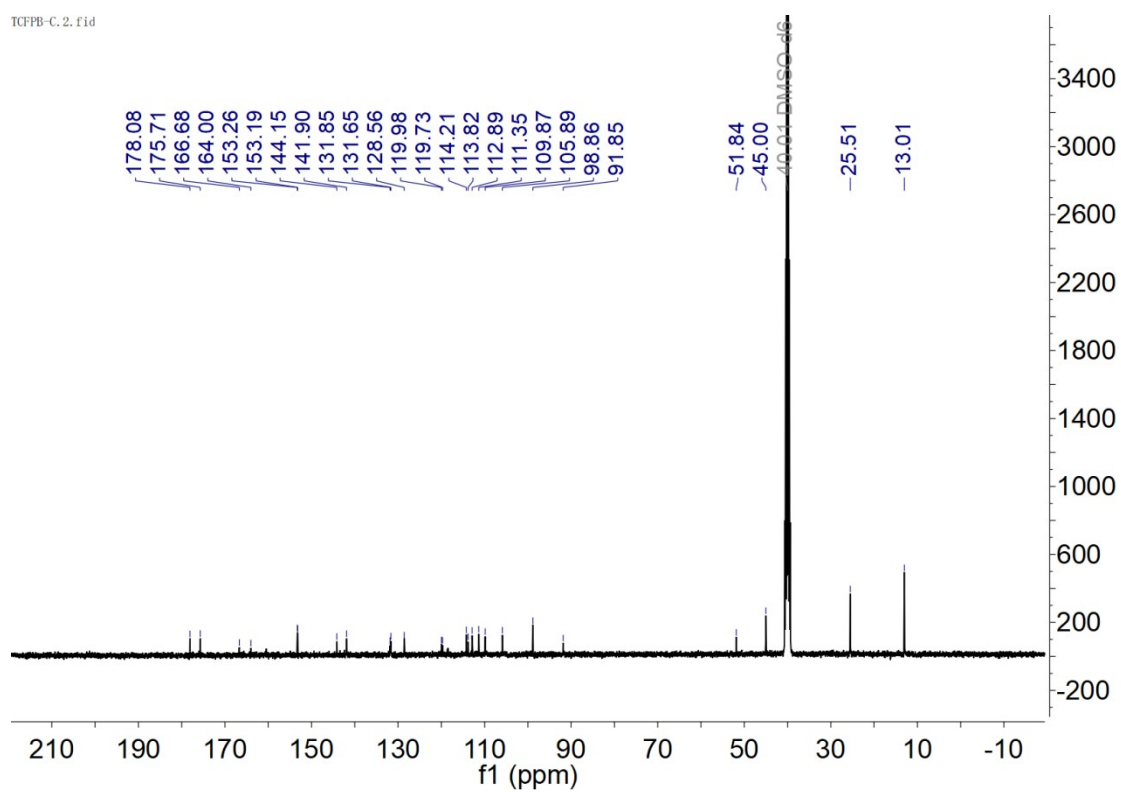


Figure S4. ^{13}C NMR spectrum of TCFPB- H_2S_n in d_6 -DMSO.

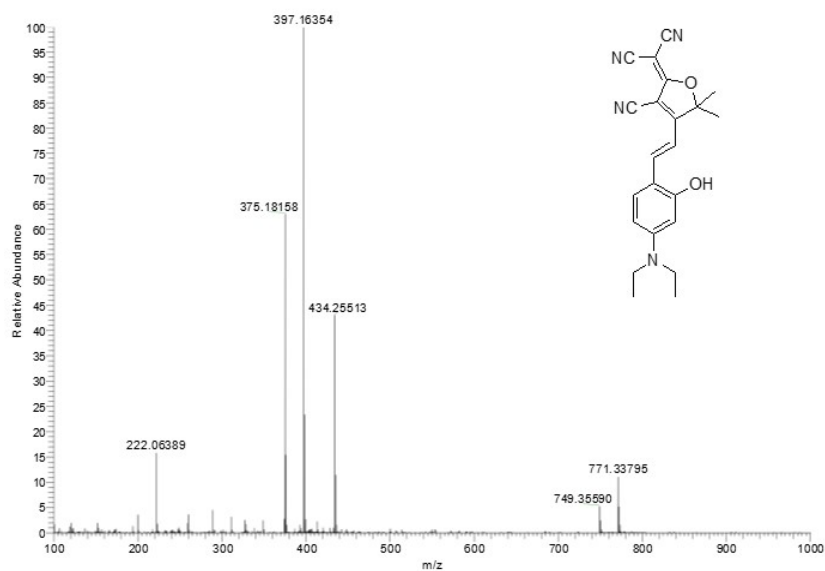


Figure S5. HRMS spectrum of TCFIS.

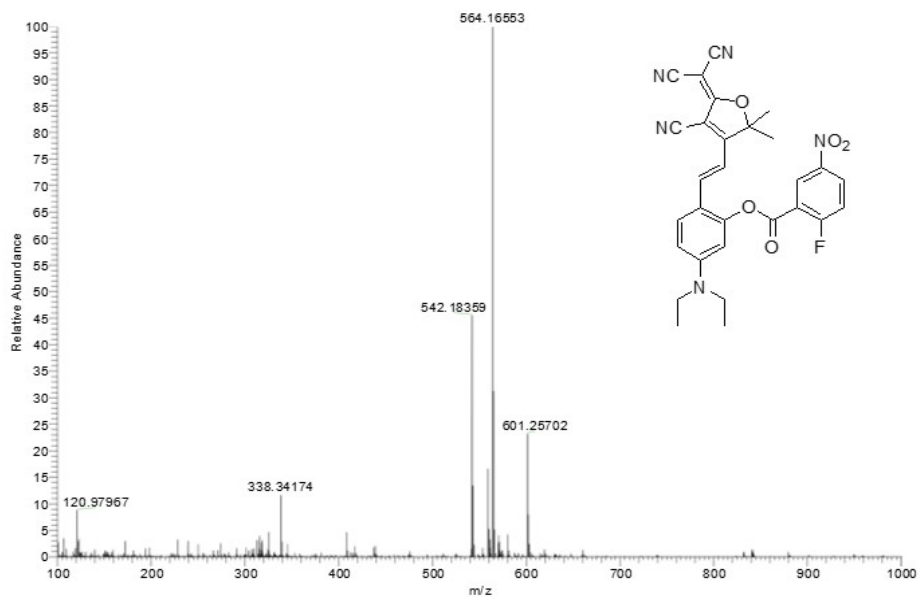


Figure S6. HRMS spectrum of TCFPB-H₂S_n.

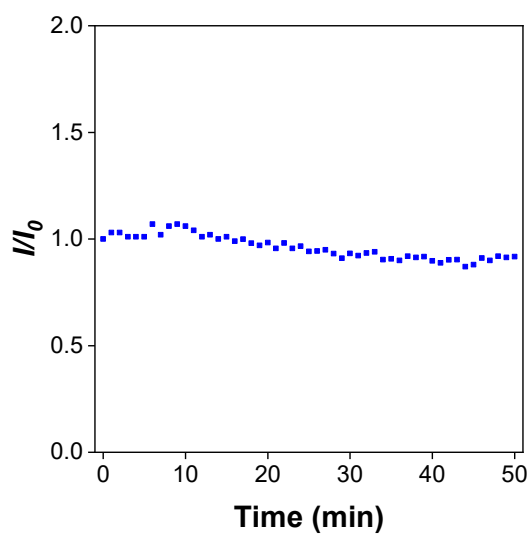


Figure S7. The light stability test of TCFPB-H₂S_n in 50 min, TCFPB-H₂S_n = 5 μM. λ_{ex} = 575 nm.

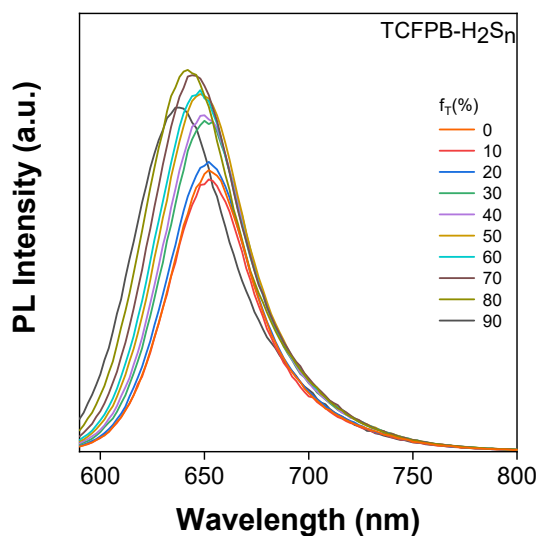


Figure S8. PL spectra of TCFPB-H₂S_n in toluene/DMSO mixtures with different toluene fractions. $\lambda_{\text{ex}} = 575$ nm.

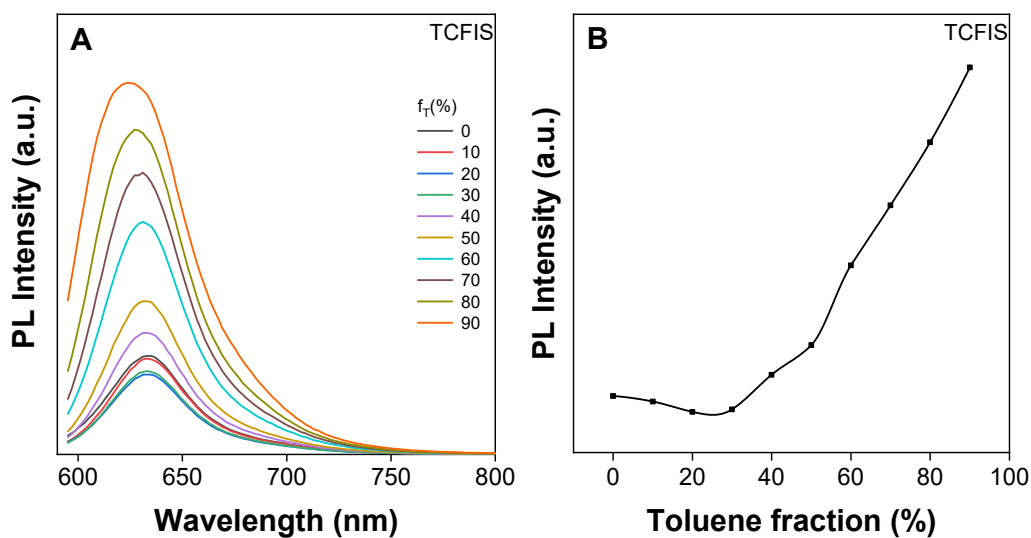


Figure S9. (A) PL spectra of TCFIS in toluene/DMSO mixtures with different toluene fractions. (B) The plot of PL intensity vs the composition of the DMSO/Toluene mixtures of TCFIS. $\lambda_{\text{ex}} = 575$ nm.



Figure S10. Fluorescence imaging for powder of TCFIS and TCFPB-H₂S_n under IVIS. Fluorescent emission was collected from 600 to 840 nm. $\lambda_{\text{ex}} = 570$ nm.

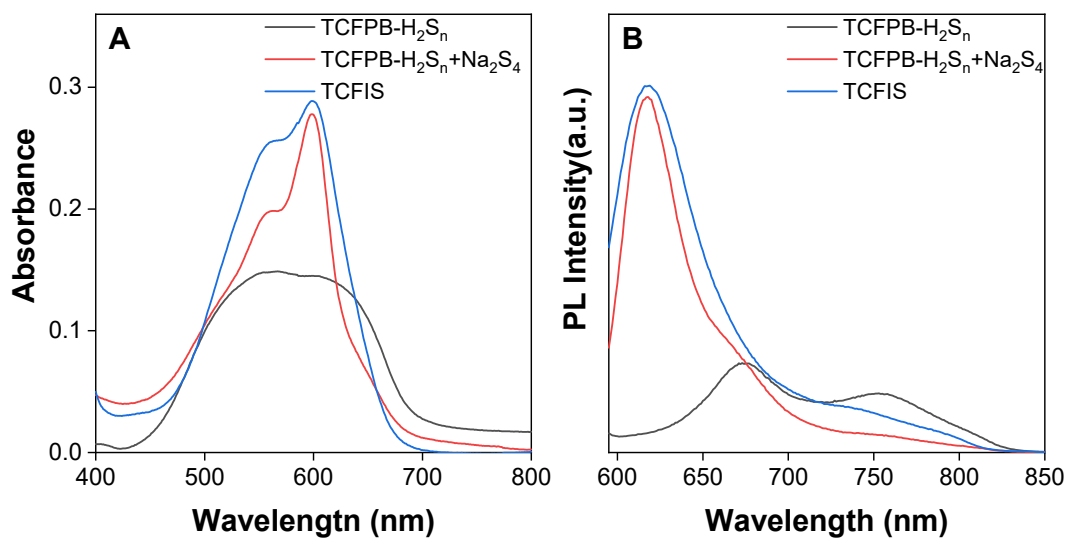


Figure S11. Normalized absorption and PL spectra of **TCFPB-H₂S_n** (5 μM, black), **TCFIS** (5 μM, blue) and **TCFPB-H₂S_n** (5 μM) after incubation with Na₂S₄ (250 μM, red) at 37°C for 5 min in PBS solution. λ_{ex} = 575 nm.

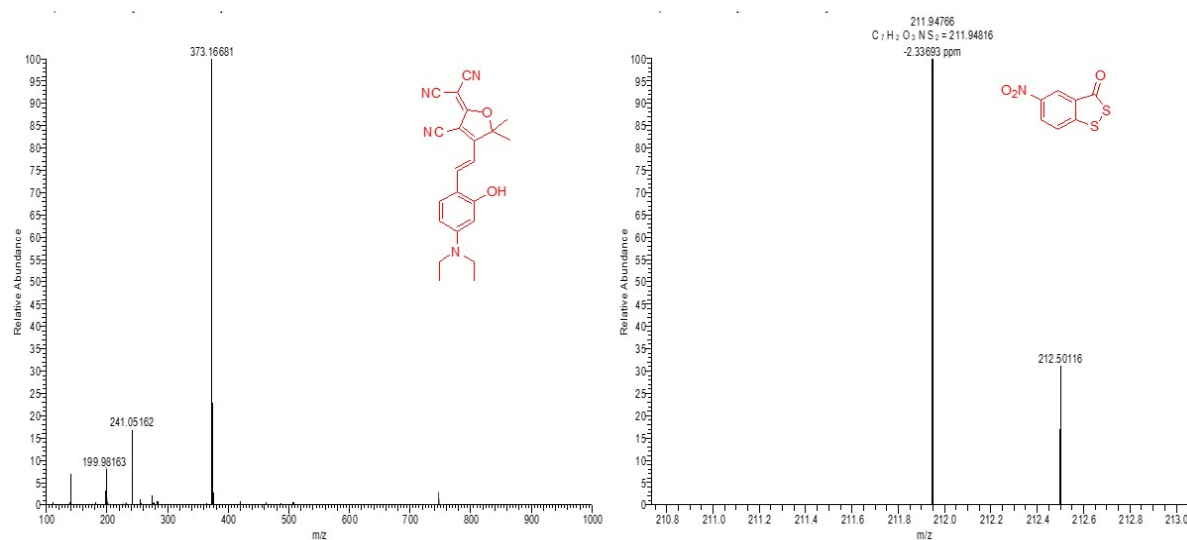


Figure S12. HRMS spectrum of **TCFPB-H₂S_n** after incubation with Na₂S₄ (300 μM) at 37 °C for 30 min. **TCFIS** ([M-H]⁻ calcd for C₂₂H₂₁N₄O₂: 373.16700, found: 373.16681). **Compound 3** ([M-H]⁻ calcd for C₇H₂NO₃S₂: 211.94816, found: 211.94766).

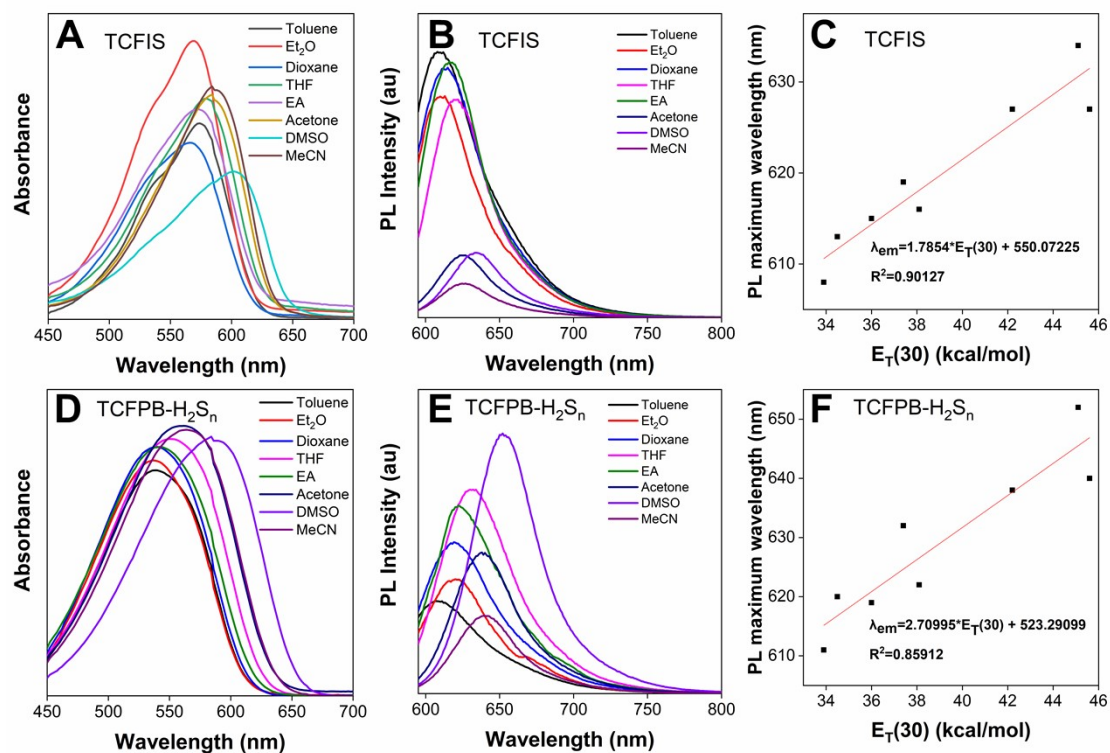


Figure S13. Absorption (A) and emission (B) spectra of **TCFIS** in different solvents. (C) Plot of the emission maximum of **TCFIS** in different solvents versus $E_T(30)$. Absorption (D) and emission (E) spectra of **TCFPB-H₂S_n** in different solvents. (F) Plot of the emission maximum of **TCFPB-H₂S_n** in different solvents versus $E_T(30)$. $E_T(30)$ was the empirical parameter for solvent polarity.

Concentration: 5 μ M. $\lambda_{ex} = 575$ nm.

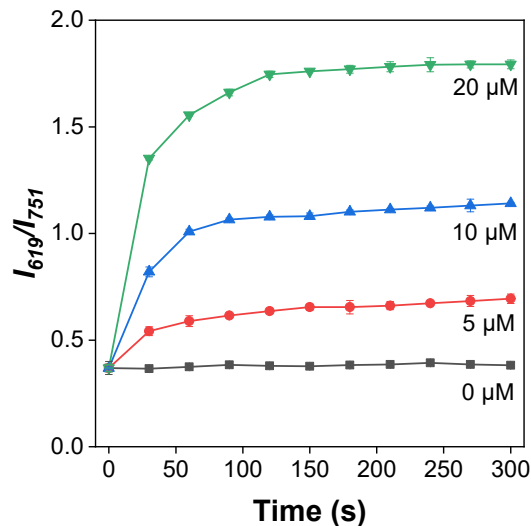


Figure S14. Time-dependent fluorescence intensity ratio (I_{619}/I_{751}) of **TCFPB-H₂S_n** (5 μ M) with different concentrations (0, 5, 10 and 20 μ M) of Na₂S₄. $\lambda_{ex} = 575$ nm.

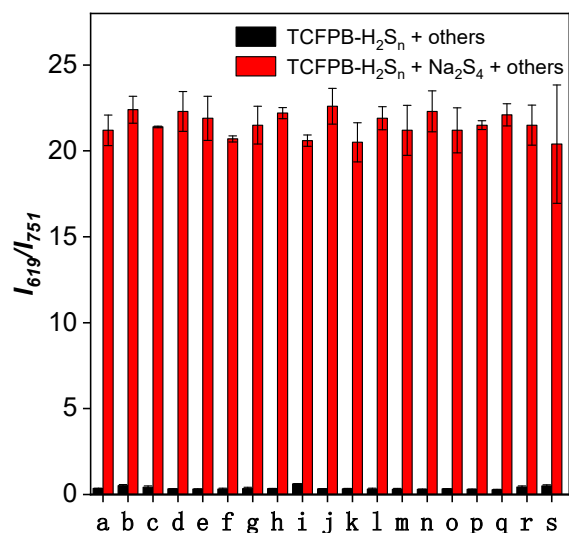


Figure S15. Fluorescence intensity ratio of I_{619}/I_{751} in the absence (black bar) or presence (red bar) of 250 μM Na_2S_4 upon addition of 250 μM other biologically-relevant species; a: $\text{S}_2\text{O}_5^{2-}$; b: ClO^- ; c: H_2O_2 ; d: MnO_4^- ; e: Mg^{2+} ; f: K^+ ; g: Cys; h: Fe^{3+} ; i: H_2S ; j: HSO_3^- ; k: SO_4^{2-} ; l: Hcy; m: I⁻; n: $\bullet\text{OH}$; o: ATP; p: $\text{S}_2\text{O}_8^{2-}$; q: GSH (5 mM); r: NO_3^- ; s: GSSH. **TCFPB-H₂S_n** = 5 μM , λ_{ex} = 575 nm.

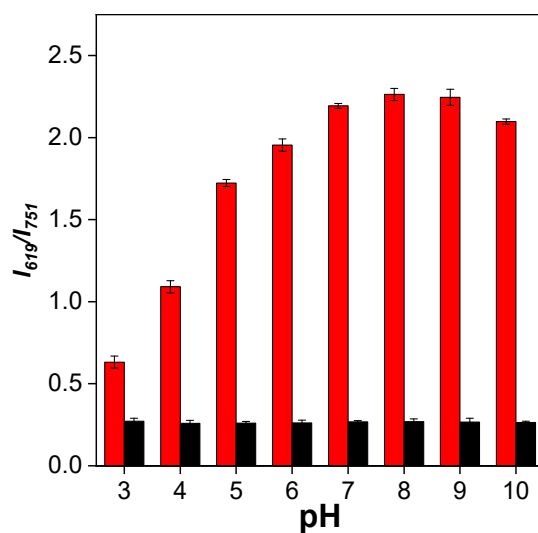


Figure S16. The PL intensity ratios (I_{619}/I_{751}) of **TCFPB-H₂S_n** (5 μM , black bars) and **TCFPB-H₂S_n** (5 μM) + Na_2S_4 (50 μM , red bars) in different pH buffers. λ_{ex} = 575 nm.

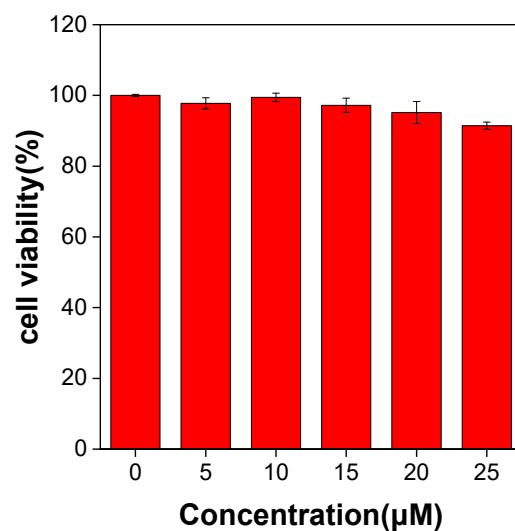


Figure S17. Cell viability of HeLa cells at varied concentrations of TCFPB- H_2S_n by using CCK8 method.

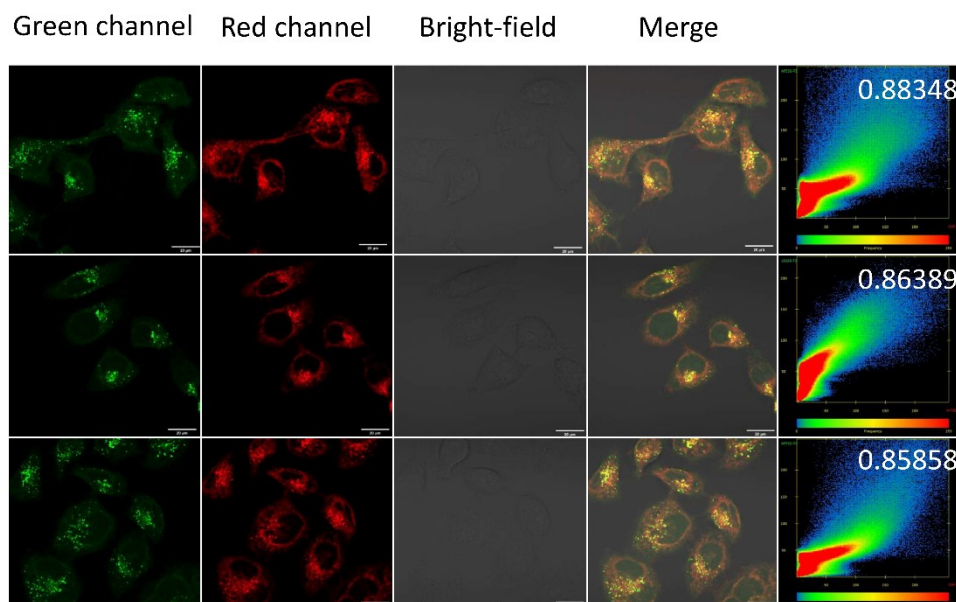


Figure S18. Colocation fluorescence image. HeLa cells were co-incubated with TCFIS ($1 \mu\text{M}$) and Lyso-tracker (100 nM) for 20 min. Lyso-tracker: green channel; TCFIS: red channel; Green channel ($500\text{--}590 \text{ nm}$), $\lambda_{\text{ex}} = 488 \text{ nm}$; red channel ($600\text{--}650 \text{ nm}$), $\lambda_{\text{ex}} = 561 \text{ nm}$. Scale bar $20 \mu\text{m}$.

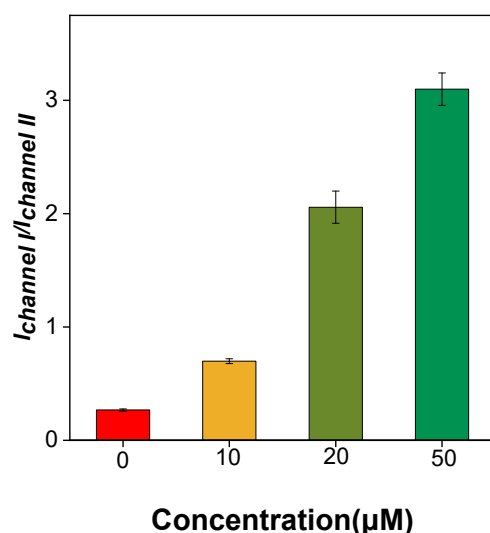


Figure S19. The PL intensity ratios ($I_{\text{channel I}} / I_{\text{channel II}}$) of the channel I and channel II in Figure 5. $\lambda_{\text{ex}} = 561 \text{ nm}$. channel I: 600-650 nm; channel II: 730-770 nm.

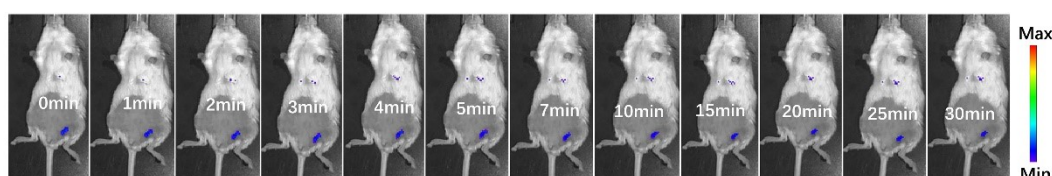


Figure S20. Time-dependent fluorescent images in live mice using probe **TCFPB- H_2S_n** in the absence of exogenous H_2S_n ; **TCFPB- H_2S_n** ($5 \mu\text{M}$, $100 \mu\text{L}$) was injected in a subcutaneous manner, followed by an injection of PBS ($100 \mu\text{L}$). Fluorescent emission was collected from 600 to 650 nm. $\lambda_{\text{ex}} = 570 \text{ nm}$.

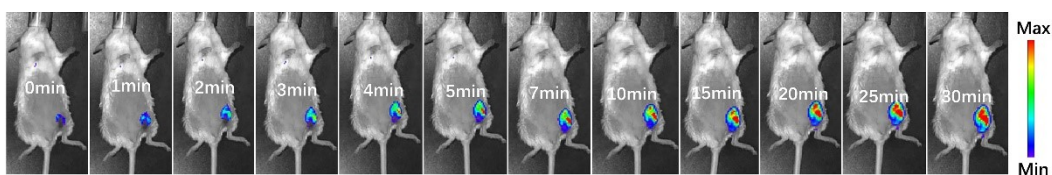


Figure S21. Time-dependent fluorescent images of H_2S_n in live mice using probe **TCFPB- H_2S_n** in the presence of exogenous H_2S_n ; **TCFPB- H_2S_n** ($5 \mu\text{M}$, $100 \mu\text{L}$) was injected, followed by an injection of Na_2S_4 (1 mM , $100 \mu\text{L}$). Fluorescent emission was collected from 600 to 650 nm. $\lambda_{\text{ex}} = 570 \text{ nm}$.

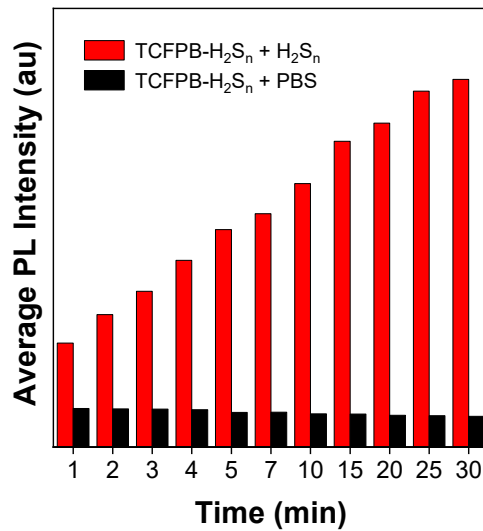


Figure S22. Time-dependent changes of average PL intensity in Figure S20 and S21.

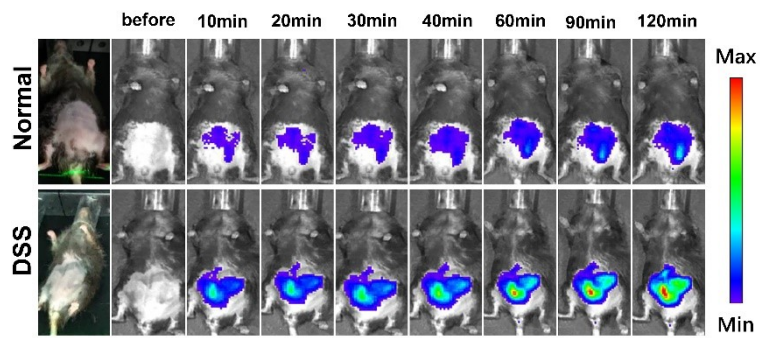


Figure S23. Time-dependent fluorescent images in live mice using probe **TCFPB-H₂S_n** in DSS and normal mice. **TCFPB-H₂S_n** (1 μ M, 100 μ L); Channel I: 600-650nm. λ_{ex} = 570 nm.

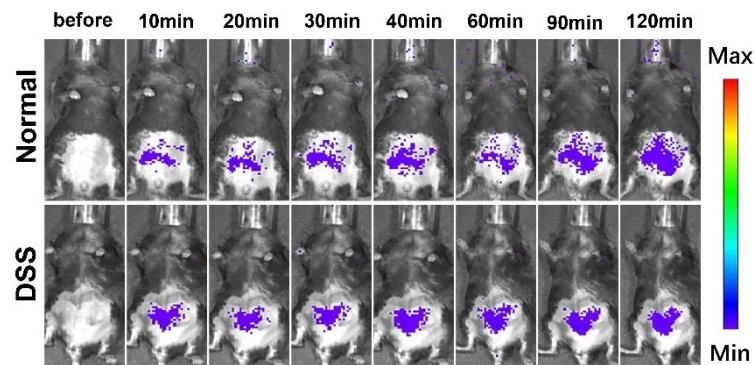


Figure S24. Time-dependent fluorescent images in live mice using probe **TCFPB-H₂S_n** in DSS and normal mice. **TCFPB-H₂S_n** (1 μ M, 100 μ L); Channel II: 730-770nm. λ_{ex} = 570 nm.

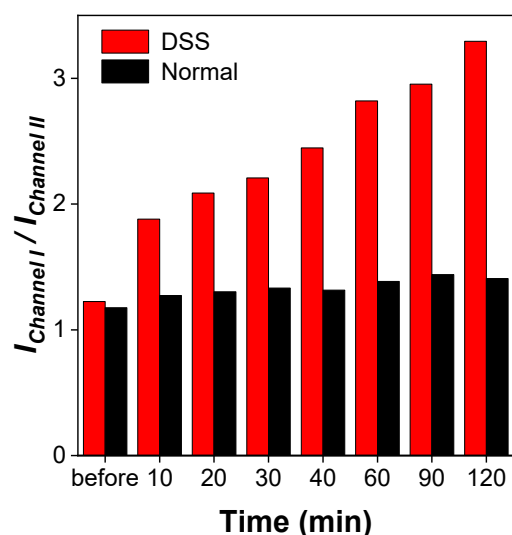


Figure S25. Time-dependent changes of average PL intensity ratios ($I_{\text{Channel I}}/I_{\text{Channel II}}$) in Figure S23 and S24.

Table S1. Comparison of reported fluorescent probes for H_2S_n detection.

References	Response time	Response mode	Detection limit	$\lambda_{\text{ex}}/\lambda_{\text{em}}$ (nm)	Targeting	Diseases <i>in vivo</i> model
Org. Lett. 2015, 17 , 2776-2779.	15 min	Turn-on (ACQ)	300 nM	350/530	/	/
Anal. Chem. 2015, 87 , 3004-3010.	ND	Turn-on (ACQ)	500 nM	730(Two-photon)/536	/	/
Analyst 2015, 140 , 3766-3772.	20 min	Turn-on (ACQ)	50 nM	707/737	/	/
Sensor Actuat B-Chem. 2016, 230 , 773-778.	10 min	Turn-on (ACQ)	152 nM	450/512	/	/
RSC. Adv. 2016, 6 , 88519-88525.	40 min	Turn-on (ACQ)	75 nM	560/620	/	/
Chem. Commun. 2017, 53 , 8759-8762.	10 min	Turn-on (ACQ)	35 nM	680/708	/	/
J. Mater. Chem. B. 2017, 5 , 2574-2579.	5 min	Turn-on (ACQ)	22 nM	680/720	/	/

Anal. Chem. 2017, 89 , 12984-12991.	60 min	Turn-on (ACQ)	40 nM	366/465	/	/
Chem. Commun. 2017, 53 , 1064-1067.	1 min	Turn-on (ACQ)	420 nM	470/525	/	/
Talanta 2017, 164 , 529-533.	7 min	Turn-on (ACQ)	18.2 nM	400/490	/	/
Anal. Chem. 2019, 91 , 7774-7791.	5 min	Turn-on (ACQ)	100 nM	500/635	/	Acute peritonitis and tumor
Anal. Chem. 2018, 90 , 881-887.	1 min	Turn-on (ACQ)	50 nM	460/490	/	/
Sensor Actuat B-Chem. 2018, 254 , 222-226.	6 min	Turn-on (ACQ)	8.2 nM	535/682	/	/
Biomater Sci 2018, 6 , 672-682.	2 min	Turn-on (ACQ)	10 nM	710/736	/	/
J. Am. Chem. Soc. 2014, 136 , 7257-7260.	5 min	Turn-on (ACQ)	71 nM	490/515	/	/
Anal. Chem. 2015, 87 , 3631-3638.	0.5 min	Turn-on (ACQ)	25 nM	675/730	Mitochondria	/
Anal. Chem. 2016, 88 , 4122-4129.	15 min	Turn-on (ACQ)	80 nM	730/780	Mitochondria	Acute liver injury
ACS. Sens. 2018, 3 , 1622-1626.	50 min	Turn-on (ACQ)	150 nM	460/520	Mitochondria	/
Anal. Chem. 2016, 88 , 7206-7212.	5 min	Ratiometric (ACQ)	100 nM	370/ 460	/	/
Sensor Actuat B-Chem. 2019, 283 , 810-819	5 min	Ratiometric (ACQ)	100 nM	372/506	Mitochondria	/
Chemical Science 2020, 11 , 7991-7999.	<1 min	Ratiometric (ACQ)	9.4 nM	420/ 486	/	/
Dyes Pigm.,2020, 172 , 107818.	3min	Ratiometric (ACQ)	21 nM	420/ 468	/	/

ACS Applied Bio Materials 2019, 2 , 1987-1997.	10 min	Ratiometric (ACQ)	10 nM	405/ 546	Mitochondria	/
Dyes Pigm., 2021, 188 ,109190.	10 min	Ratiometric (ACQ)	20 nM	405/ 550	Mitochondria	/
Anal. Chim. Acta. 2019, 1056 , 117-124.	6 min	Turn-on (ACQ)	84 nM	340/520	Lysosome	/
Biomater Sci 2020, 8 , 224-231.	1 min	Turn-on (ACQ)	1 nM	300/478	Lysosome	/
Dyes Pigm., 2020, 173 ,107877.	5 min	Ratiometric (ACQ)	10 nM	405/ 548	Lysosome	/
This work	2 min	Ratiometric(AIE)	43 nM	575/ 619	Lysosome	Acute ulcerative colitis

References:

- 1 Julian Tirado-Rives and William L. Jorgensen, Performance of B3LYP Density Functional Methods for a Large Set of Organic Molecules, *J. Chem. Theory Comput.* 2008, **4**, 297–306.
- 2 Tariq Mahmood, Naveen Kosar, Khurshid Ayub, DFT study of acceleration of electrocyclization in photochromes under radical cationic conditions: Comparison with recent experimental data, *Tetrahedron.*2017, **73**, 3521–3528.